

## Spin Waves in a Bose-Einstein–Condensed Atomic Spin Chain

Weiping Zhang, Han Pu, Chris Search, and Pierre Meystre

*Optical Sciences Center, The University of Arizona, Tucson, Arizona 85721*

(Received 21 September 2001; published 25 January 2002)

The spin dynamics of atomic Bose-Einstein condensates confined in a one-dimensional optical lattice is studied. The condensates at each lattice site behave like spin magnets that can interact with each other through both the light-induced dipole-dipole interaction and the static magnetic dipole-dipole interaction. We show how these site-to-site dipolar interactions can distort the ground-state spin orientations and lead to the excitation of spin waves. The dispersion relation of the spin waves is studied and possible detection schemes are proposed.

DOI: 10.1103/PhysRevLett.88.060401

PACS numbers: 03.75.Fi, 75.45.+j, 75.60.Ej

Rapid experimental progress in the realization of trapped degenerate quantum atomic gases has generated fascinating opportunities to study a wide range of physical phenomena in atomic physics, condensed matter physics, and quantum optics. In particular, the recent success in all-optical confinement [1,2] and formation [3] of atomic Bose-Einstein condensates provides a unique tool to explore the magnetic properties and spin-dependent dynamics of ultracold atomic gases [4]. In this Letter, we propose a scheme to study the excitation and propagation of spin waves in an array of atomic spinor Bose-Einstein condensates confined or created in an optical lattice.

Spin-wave phenomena play an important role in solid state physics [5]. In solids, spin-wave excitations result from the exchange interaction of electrons between atoms in the crystal. They are usually associated with spin-1/2 Fermi systems with an effective interaction range of a few angstroms, a typical lattice period in solid materials. Although the Bose-Einstein–condensed atoms in optical lattices exhibit a number of close analogies to atoms in a real crystal, a number of differences exist. (i) The atomic spacing in an optical lattice is of the order of half an optical wavelength and as such is much larger than a crystal lattice period. (ii) As a result, the electron exchange interaction is completely negligible: spin waves, if they exist,

must be caused by other forms of long range interactions. (iii) There is a large number of (bosonic) atoms at each lattice site, typically of the order of 1000 or more, and they are subject to Bose-enhancement effects. As a result of these differences, the Bose condensates in an optical lattice offer a totally new environment to study spin dynamics in periodic structures.

The schematic diagram of Fig. 1 shows the system discussed in this Letter. We consider for concreteness a one-dimensional (1D) optical lattice formed by two  $\pi$ -polarized laser beams counterpropagating along the  $y$  axis. We assume that, in the  $x$ - $z$  plane, Bose-Einstein–condensed alkali atoms in their hyperfine ground-state manifold are tightly confined by an optical dipole potential arising from either the transverse profile of the lattice field or from a separate laser. Hence a 1D coherent atomic chain is formed along the  $y$  axis. We employ a spinor atomic field theory to describe the interaction of the atoms with the lattice laser beams. For large detunings  $\Delta = \omega_L - \omega_a$  between the frequency  $\omega_L$  of the laser fields and the atomic transition frequency  $\omega_a$  it is possible to adiabatically eliminate the excited atomic state field operator. The resulting Heisenberg equations of motion for the hyperfine ground-state atomic field operators  $\hat{\psi}_m(\mathbf{r}, t)$ , including interatomic collisions and static magnetic dipole-dipole interaction, take the form [6–9]

$$i\hbar \frac{\partial \hat{\psi}_m}{\partial t} = \left[ -\frac{\hbar^2 \nabla^2}{2m} + V_L \right] \hat{\psi}_m + \sum_{m', n'} \int d\mathbf{r}' [Q_{mm'n'}(\mathbf{r}, \mathbf{r}') + V_{mm'n'}^{\text{coll}}(\mathbf{r}, \mathbf{r}') + V_{mm'n'}^{\text{d-d}}(\mathbf{r}, \mathbf{r}')] \hat{\psi}_{m'}^\dagger(\mathbf{r}') \hat{\psi}_{n'}(\mathbf{r}') \hat{\psi}_n(\mathbf{r}), \quad (1)$$

where  $V_L(\mathbf{r}) = U_0 \exp[-r_\perp^2/W_L^2] \cos^2(k_L y)$  is the light-induced lattice potential, with  $r_\perp \equiv \sqrt{x^2 + z^2}$ ,  $k_L = 2\pi/\lambda_L$  the wave number, and  $W_L$  the width of the lattice beams. The potential depth is defined as  $U_0 = \hbar|\Omega|^2/6\Delta$  with  $\Omega$  being the Rabi frequency. The index  $m = -F, \dots, F$  denotes the Zeeman sublevels of the electronic ground state of the atoms with angular momentum  $F$ . In this Letter we take  $F = 1$  for the ground-state alkali atoms.

The first nonlinear term in Eq. (1) originates from the photon-exchange interaction between the condensed atoms. It describes the light-induced dipole-dipole interaction and is characterized by the quantity

$$Q_{mm'n'}(\mathbf{r}, \mathbf{r}') = 3 \frac{\gamma}{\Delta} U_0 \exp\left(-\frac{r_\perp^2 + r_\perp'^2}{W_L^2}\right) \cos(k_L y) \cos(k_L y') \\ \times \left[ \frac{4}{9} \delta_{m'n'} \delta_{mn} \mathbf{e}_0 \cdot \mathbf{W}(\mathbf{r} - \mathbf{r}') \cdot \mathbf{e}_0 - \mathbf{d}_{m'n'} \cdot \mathbf{W}(\mathbf{r} - \mathbf{r}') \cdot \mathbf{d}_{mn} \right],$$

where  $\gamma$  is the single-atom spontaneous emission rate and  $\mathbf{d}_{mn} = (F_{mn}^{(+)}\mathbf{e}_{-1} + F_{mn}^{(-)}\mathbf{e}_{+1})/6\hbar$  denotes the dipole moments induced by the  $\pi$ -polarized light fields. Here,  $F_{mn}^{(\pm)}$  are the matrix elements of the “+” and “-” components of the total angular momentum operator  $\mathbf{F}$ , and  $\mathbf{e}_{\pm 1,0}$  are unit vectors in the spherical harmonic basis. The tensor  $\mathbf{W}$ , describing the spatial profile of the light-induced dipole-dipole interaction, has the form

$$\mathbf{W}(\mathbf{r}) = \frac{3}{4} \left[ (\mathbf{11} - 3\hat{\mathbf{r}}\hat{\mathbf{r}}) \left( \frac{\sin\xi}{\xi^2} + \frac{\cos\xi}{\xi^3} \right) - (\mathbf{11} - \hat{\mathbf{r}}\hat{\mathbf{r}}) \frac{\cos\xi}{\xi} \right],$$

where  $\mathbf{11}$  is the unit tensor,  $\mathbf{r} = \mathbf{r}/|\mathbf{r}|$ , and  $\xi = k_L|\mathbf{r}|$ .

The two-body ground-state collisions and magnetic dipole-dipole interaction are described by the potentials

$$V_{mm'n'n}^{\text{coll}}(\mathbf{r}, \mathbf{r}') = [\lambda_s \delta_{m'n'} \delta_{mn} + \lambda_a \mathbf{F}_{mn} \cdot \mathbf{F}_{m'n'}] \delta(\mathbf{r} - \mathbf{r}'),$$

$$V_{mm'n'n}^{\text{d-d}}(\mathbf{r}, \mathbf{r}') = \frac{\mu_0 \mu_B^2 g_F^2}{4\pi |\mathbf{r} - \mathbf{r}'|^3} \left[ \mathbf{F}_{mn} \cdot \mathbf{F}_{m'n'} - 3 \frac{\mathbf{F}_{mn} \cdot (\mathbf{r} - \mathbf{r}') \mathbf{F}_{m'n'} \cdot (\mathbf{r} - \mathbf{r}')}{|\mathbf{r} - \mathbf{r}'|^2} \right],$$

respectively, where  $\lambda_s$  and  $\lambda_a$  are related to the  $s$ -wave scattering lengths of the spinor condensate [9].

The optical potential associated with a sufficiently deep optical lattice is equivalent to a periodic array of independent “microtraps” [2]. If the depth of each of those is large enough, an array of independent Bose condensates can be formed in the lattice, and it is convenient to expand the spinor atomic field operator as  $\hat{\psi}_m(\mathbf{r}) = \sum_i \phi_i(\mathbf{r}) \hat{a}_m(i)$ , where  $\phi_i$  is the condensate wave function for the  $i$ th microtrap, and the operators  $\hat{a}_m(i)$  satisfy the bosonic commutation relations  $[\hat{a}_m(i), \hat{a}_n^\dagger(j)] = \delta_{mn} \delta_{ij}$ . For deep enough microtraps the spatial overlap between the individual condensate wave functions is negligible, and they can be considered as independent. Under this tight-binding condition, the spatial wave function of the  $i$ th condensate is then determined by the Gross-Pitaevskii (GP) equation  $[-\frac{\hbar^2 \nabla^2}{2m} + V_i(\mathbf{r}) + \lambda_s(N_i - 1)|\phi_i(\mathbf{r})|^2]\phi_i(\mathbf{r}) = \mu_i \phi_i(\mathbf{r})$ , with  $V_i(\mathbf{r}) = U_0 \exp[-r_\perp^2/W_L^2] \cos^2(k_L y + i\pi)$  for  $0 < y < \lambda_L/2$  being the potential near the  $i$ th microtrap,  $N_i = \sum_m \langle \hat{a}_m^\dagger(i) \hat{a}_m(i) \rangle$  the number of condensed atoms at the site, and  $\mu_i$  the chemical potential.

We remark that the local dipole-dipole interaction is ignored in the GP equation. Its effect on the condensate has recently been studied by a number of authors [10–12], and it may lead to an instability, depending on the geometry of the confining trap. For a pancake trap, the condensate is always stable [10] if the aspect ratio  $l = (\omega_\rho/\omega_z)^{1/2} < 0.4$ . In the case of an optical lattice, each “microtrap” is approximately pancakelike. For the range of parameters used in this paper, the aspect ratio of the microtrap falls into the stable regime. Furthermore, the atomic number

$N$  at each lattice site is small which reduces the effect of the dipole-dipole interaction [10,11]. As a result, the dipole-dipole interaction within each site can be safely ignored.

For  $F = 1$ , the individual condensates consist of atoms with three Zeeman sublevels, hence they behave as collective spin magnets in the presence of external magnetic fields. Such spin magnets form a 1D coherent spin chain along the optical lattice. Under the tight-binding approximation and ignoring both the nonresonant and spin-independent constant terms, we can construct the spin Hamiltonian from Eq. (1),

$$H = \sum_i \left[ \lambda'_a \hat{\mathbf{S}}_i^z - \gamma_B \hat{\mathbf{S}}_i \cdot \mathbf{B} - \sum_{j \neq i} J_{ij}^z \hat{\mathbf{S}}_i^z \hat{\mathbf{S}}_j^z - \sum_{j \neq i} J_{ij} (\hat{\mathbf{S}}_i^{(-)} \hat{\mathbf{S}}_j^{(+)} + \hat{\mathbf{S}}_i^{(+)} \hat{\mathbf{S}}_j^{(-)}) \right], \quad (2)$$

where we have defined the collective spin operators  $\hat{\mathbf{S}}_i = \sum_{mn} \hat{a}_m^\dagger(i) \mathbf{F}_{mn} \hat{a}_n(i)$ , with components  $\hat{S}_i^{\{\pm, z\}}$ . We have also introduced an external magnetic field  $\mathbf{B} = B_0 \mathbf{e}_0$  whose strength is strong enough to polarize the ground-state spin orientations of the atomic chain along the quantization axis  $z$  [4]. The parameter  $\gamma_B = -\mu_B g_F$  is the gyromagnetic ratio, with  $\mu_B$  being the Bohr magneton and  $g_F$  the Landé  $g$  factor.

The first term in Hamiltonian (2) results from the spin-dependent interatomic collisions at a given site, with  $\lambda'_a = (1/2)\lambda_a \int d^3 r |\phi_i(\mathbf{r})|^4$ . The last two terms describe the site-to-site spin coupling induced by both the static magnetic field and light-induced dipolar interactions. The coupling coefficients have the explicit forms

$$J_{ij}^z = \frac{\mu_0 \gamma_B^2}{16\pi \hbar^2} \int d\mathbf{r} \int d\mathbf{r}' \frac{|\mathbf{r}'|^2 - 3y'^2}{|\mathbf{r}'|^5} |\phi_i(\mathbf{r})|^2 |\phi_j(\mathbf{r} - \mathbf{r}')|^2,$$

$$J_{ij} = \frac{\gamma U_0}{24\Delta \hbar^2 k_L^3} \int d\mathbf{r} \int d\mathbf{r}' f_c(\mathbf{r}') \exp\left(-\frac{r_\perp^2 + |\mathbf{r}_\perp - \mathbf{r}'_\perp|^2}{W_L^2}\right) \cos(k_L y) \cos[k_L(y - y')] \mathbf{e}_{+1} \cdot \mathbf{W}(\mathbf{r}') \cdot \mathbf{e}_{-1} \\ \times |\phi_i(\mathbf{r})|^2 |\phi_j(\mathbf{r} - \mathbf{r}')|^2 + \frac{1}{2} J_{ij}^z, \quad (3)$$

where we have introduced a cutoff function  $f_c(\mathbf{r}) = \exp(-r^2/L_c^2)$  to describe the effective interaction range of the light-induced dipole-dipole interaction, with  $L_c = N\gamma/c$  being the coherence length associated with the collective spontaneous emission of  $N$  atoms [13].

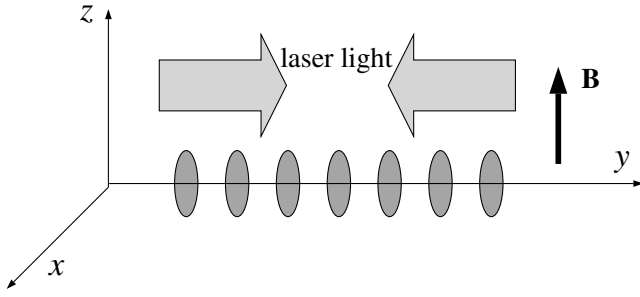


FIG. 1. Schematic diagram shows that a spinor condensate is confined in an optical lattice in the  $y$  axis with an external magnetic field along the  $z$  direction.

The physics implicit in Hamiltonian (2) is quite clear. Consider first the situation without site-to-site coupling,  $J_{ij} = 0$ . In the presence of a sufficiently strong external magnetic field, the spins align themselves along the quantization axis  $z$ . For ferromagnetic condensates, as in the case of  $^{87}\text{Rb}$  ( $\lambda'_a < 0$ ) [14,15] (or in the presence of a strong external magnetic field for antiferromagnetic condensates), the ground state of the Hamiltonian is  $|GS\rangle = |N, -N\rangle$ , where  $N = \sum_i N_i$  is the total atomic number in the lattice. The total spin at site  $i$  has the expectation value  $\langle \hat{S}_i^z \rangle = -N_i \hbar$ , where the factor  $N_i$  is due to Bose enhancement.

For  $J_{ij} \neq 0$ , the situation changes drastically: the transfer of transverse spin excitation from site to site is allowed, resulting in the distortion of the ground-state spin structure. This distortion can propagate and hence generate spin waves along the atomic spin chain. From Hamiltonian (2), we can derive the Heisenberg equations of motion for the spin excitations as

$$i\partial \hat{S}_q^{(-)}/\partial t = (\omega_0 + \Delta\omega_q)\hat{S}_q^{(-)} - \sum_{j \neq q} \chi_{qj} \hat{S}_j^{(-)}, \quad (4)$$

where we have replaced the spin operator  $\hat{S}_q^z$  by its ground-state expectation value in the mean-field approximation.  $\omega_0 = -\gamma_B B$  and  $\Delta\omega_q = 2 \sum_{j \neq q} J_{qj}^z N_j \hbar$  determine the precessing frequency of the  $q$ th spin, while the nonzero spin-coupling coefficients  $\chi_{qj} = 2J_{qj} N_q \hbar$  give rise to the propagation of the spin waves. From Eq. (3), we observe that the light-induced dipolar interaction contributes only to spin coupling in the  $x$ - $y$  plane. This is because the  $\pi$ -polarized lattice beams induce an effective dipole moment only in that plane.

To further understand how Eq. (4) determines the existence and propagation of spin waves, it is helpful to consider the special case where the lattice is infinitely long and the spin excitations are in the long-wavelength limit. We can then reexpress Eq. (4) in its continuous limit by the replacements  $\hat{S}_q^{(-)} \rightarrow S(y, t)$ ,  $\chi_{qj} \rightarrow \chi(y - y')$ , and  $(\omega_0 + \Delta\omega_q) \rightarrow \omega(y)$ ,

$$i \frac{\partial S(y, t)}{\partial t} = \omega(y) S(y, t) - \frac{2}{\lambda_L} \int dy' \chi(y - y') S(y', t). \quad (5)$$

In the long-wavelength limit, the last integral term in Eq. (5) can be evaluated up to the second-order expansion of  $S(y', t)$ . This leads to an effective Schrödinger equation

$$i \frac{\partial S(y, t)}{\partial t} = \left[ -\frac{\beta_1}{2} \frac{\partial^2}{\partial y^2} - \beta_0 + \omega(y) \right] S(y, t), \quad (6)$$

where we have defined  $\beta_n = (2/\lambda_L) \int d\eta \chi(\eta) \eta^{2n}$  for  $n = 0, 1$ . Evidently, from Eq. (6),  $S(y, t)$  describes the “waves” caused by spin excitations in the  $x$ - $y$  plane. These waves can be associated with the center-of-mass motion of a quantum-mechanical particle of effective mass  $m = \hbar/\beta_1$ . Being similar to the phonon associated with sound waves, the excitations associated with the spin waves are usually referred to as “magnons” [5].

We can evaluate the magnon dispersion relation by solving the discrete wave equation (4) for waves of the form  $\hat{S}_q^{(-)} = \hat{a}_k \exp[-i(\omega_0 + \Delta\omega_0 - 2 \sum_{j>0} \chi_{0j})t] \times \exp[i(kq\lambda_L/2 - \omega_k t)]$ . For simplicity, we assume a lattice with each site having the same number of atoms,  $N_i = N_0$ . This yields the dispersion relation

$$\omega_k = 2 \sum_{j>0} \chi_{0j} [1 - \cos(jk\lambda_L/2)], \quad (7)$$

where we have taken  $q = 0$  in the coefficients of Eq. (4) since their values are independent of  $q$  in the case at hand as long as we have a sufficient number of lattice sites.

Figure 2 shows the magnon dispersion spectrum and its dependence on the transverse width  $w$  of the Bose-Einstein–condensates. As  $w$  increases, the dipolar interactions among atoms tend to cancel each other, thereby

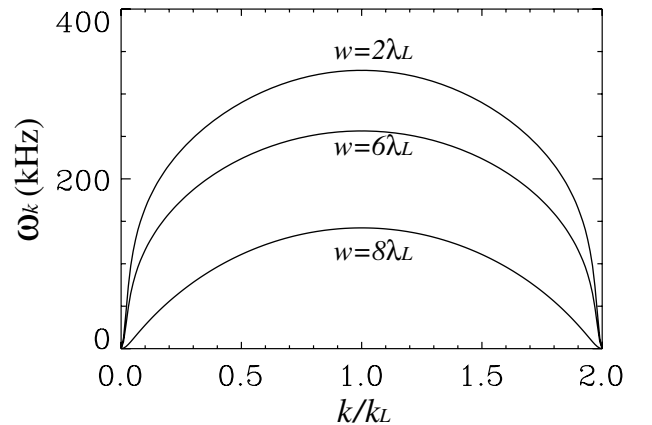


FIG. 2. Magnon dispersion spectrum. In the calculation, we have assumed that the spatial dimension along the  $y$  axis of the condensate in each lattice site is much less than  $\lambda_L$ , while, in the transverse ( $x$ - $z$ ) plane, the condensate has a Gaussian shape with a width  $w$ . We have taken  $\lambda_L = 1 \mu\text{m}$  and  $\gamma|\Omega|^2/\Delta^2 = 10^3$  and used a total number of 100 lattice sites with 2000 atoms in each site.

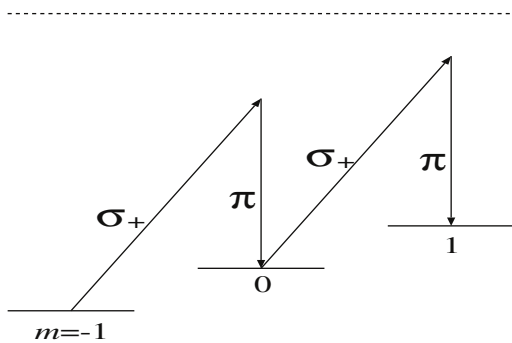


FIG. 3. Magnon detection schemes.

reducing the excitation frequency of the spin waves. As a result, it becomes difficult to excite the spin waves in the coherent atomic chain through the dipole-dipole interaction for condensate widths much larger than one optical wavelength. In addition, our numerical calculations show that for typical experimental parameters the strength of the light-induced dipolar interaction dominates over the magnetic dipolar interaction in the determination of the coupling coefficients  $\chi_{0j}$ .

Having established the existence of spin waves in condensate lattices, it remains to determine how to detect them. Any optical or magnetic method which can excite the internal transitions between the atomic Zeeman sublevels can be used for this purpose. On the other hand, the detection scheme should be able to distinguish different spin wave modes (see discussion below). A natural choice consists of employing Raman transitions, as shown in Fig. 3. The coupling of the Zeeman sublevels produced from the Raman beams exactly creates the spin transition associated with the operators  $\hat{S}^{(\pm)}$ . The existence of spin waves can then be detected by measuring the absorption of one of the Raman beams. The absorption spectrum is proportional to the sum of the transition probabilities among the Zeeman sublevels,

$$P \propto \sum_k \frac{|\langle \Phi_k | S_q^+ | GS \rangle|^2}{2} \frac{\sin^2[(\nu - \omega_p - \omega_k)\tau/2]}{[(\nu - \omega_p - \omega_k)\tau/2]^2},$$

where the kets  $|\Phi_k\rangle$  denote excited states with spin waves of frequency  $\omega_k$ ,  $\nu$  is the frequency difference between the two Raman beams,  $\tau$  is the measurement time, and  $\omega_p = \omega_0 + \Delta\omega_0 - 2\sum_{j>0}\chi_{0j}$  defines the total spin precessing frequency. Absorption resonances occur whenever the frequency  $\nu$  is tuned to match a spin-wave frequency  $\omega_k$ . For an infinitely long lattice, this will produce a broadened absorption spectrum whose width characterizes the existence of spin waves. In practice, though, the optical lattice is finite with length  $L$ . Such lattices allow only the excitation of spin waves with discrete wave numbers resulting from the resonance excitation condition  $kL = n\pi$ ,  $k$  being the wave number of the spin waves in Eq. (7). As a result, the absorption spectrum will exhibit a multippeak structure. In the long-wavelength limit, the interval between peaks

is proportional to  $\Delta\omega_k \approx (2n - 1)(\pi/N_L)^2 \sum_{j>0} \chi_{0j} j^2$ , with  $N_L$  being the total number of lattice sites.

In current experiments in optical lattices,  $N_L$  is in the range of  $\sim 10$ – $100$ , and each lattice site can accommodate a few thousand atoms. This leads to a requirement for the frequency measurement precision of about  $\sim 10$ – $100$  kHz. This is achievable with current techniques.

Alternatively, one can also carry out measurements in momentum space. The magnons associated with spin waves of wave number  $k$  have momenta  $\mathbf{p} = \hbar k \mathbf{e}_y$ . If one observes the Raman scattering using two Raman beams through the Bose gas, the momentum conservation between the magnons and Raman photons requires  $\Delta\mathbf{k} = k\mathbf{e}_y$  with  $\Delta\mathbf{k}$  being the difference of wave vectors between two Raman beams. Hence the momentum distribution of the scattered Raman photons can identify the existence of the spin waves.

In conclusion, Bose condensates in an optical lattice offer a new tool and test ground to study the quantum spin phenomena. The Bose statistics in each lattice site makes the atoms behave like a spin magnet. Such spin magnet arrays not only exhibit fascinating spin dynamics as shown in this Letter, but also may find potential applications in quantum information and computation.

We thank Dr. B. P. Anderson for several enlightening discussions concerning the detection of magnons. This work is supported in part by the U.S. Office of Naval Research under Contract No. 14-91-J1205, by the National Science Foundation under Grant No. PHY98-01099, by the U.S. Army Research Office, by NASA, and by the Joint Services Optics Program.

- 
- [1] B. P. Anderson and M. A. Kasevich, *Science* **282**, 1686 (1998); C. Orzel *et al.*, *Science* **291**, 2386 (2001).
  - [2] M. Greiner, cond-mat/0105105.
  - [3] M. D. Barrett, J. A. Sauer, and M. S. Chapman, *Phys. Rev. Lett.* **87**, 010404 (2001).
  - [4] H. Pu, Weiping Zhang, and P. Meystre, *Phys. Rev. Lett.* **87**, 140405 (2001).
  - [5] See, for example, C. Kittel, *Quantum Theory of Solids* (Wiley, New York, 1987).
  - [6] Weiping Zhang and D. F. Walls, *Phys. Rev. A* **49**, 3799 (1994); *ibid.* **57**, 1248 (1998).
  - [7] T.-L. Ho, *Phys. Rev. Lett.* **81**, 742 (1998).
  - [8] T. Ohmi and K. Machida, *J. Phys. Soc. Jpn.* **67**, 1882 (1998).
  - [9] C. K. Law, H. Pu, and N. P. Bigelow, *Phys. Rev. Lett.* **81**, 5257 (1998).
  - [10] L. Santos *et al.*, *Phys. Rev. Lett.* **85**, 1791 (2000).
  - [11] K. Goral, K. Rzazewski, and T. Pfau, *Phys. Rev. A* **61**, 051601(R) (2000).
  - [12] S. Yi and L. You, *Phys. Rev. A* **63**, 053607 (2001).
  - [13] J. Javanainen, *Phys. Rev. Lett.* **72**, 2375 (1994).
  - [14] D. Heinzen (private communication).
  - [15] J. P. Burke, Jr., and J. L. Bohn, *Phys. Rev. A* **59**, 1303 (1999); N. N. Klausen, J. L. Bohn, and C. H. Greene, *Phys. Rev. A* **64**, 053602 (2001).